PHILOSOPHICAL TRANSACTIONS OF THE ROYAL SOCIETY A

Phil. Trans. R. Soc. A (2007) **365**, 1867–1888
doi:10.1098/rsta.2007.2047
Published online 18 May 2007

Anaerobic methanotrophy and the rise of atmospheric oxygen

By D. C. Catling[1,2,*], M. W. Claire[3] and K. J. Zahnle[4]

[1]*Department of Earth Sciences, University of Bristol, Wills Memorial Building, Queen's Road, Bristol BS8 1RJ, UK*
[2]*Astrobiology Program and Department of Atmospheric Sciences, University of Washington, Box 351640, Seattle, WA 98195, USA*
[3]*Astrobiology Program and Department of Astronomy, University of Washington, Box 351580, Seattle, WA 98195, USA*
[4]*Mail Stop 245-3, Space Science Division, NASA Ames Research Centre, Moffett Field, CA 94035, USA*

In modern marine sediments, the anoxic decomposition of organic matter generates a significant flux of methane that is oxidized microbially with sulphate under the seafloor and never reaches the atmosphere. In contrast, prior to *ca* 2.4 Gyr ago, the ocean had little sulphate to support anaerobic oxidation of methane (AOM) and the ocean should have been an important methane source. As atmospheric O_2 and seawater sulphate levels rose on the early Earth, AOM would have increasingly throttled the release of methane. We use a biogeochemical model to simulate the response of early atmospheric O_2 and CH_4 to changes in marine AOM as sulphate levels increased. Semi-empirical relationships are used to parameterize global AOM rates and the evolution of sulphate levels. Despite broad uncertainties in these relationships, atmospheric O_2 concentrations generally rise more rapidly and to higher levels (of order approx. 10^{-3} bar versus approx. 10^{-4} bar) as a result of including AOM in the model. Methane levels collapse prior to any significant rise in O_2, but counter-intuitively, methane re-rises after O_2 rises to higher levels when AOM is included. As O_2 concentrations increase, shielding of the troposphere by stratospheric ozone slows the effective reaction rate between oxygen and methane. This effect dominates over the decrease in the methane source associated with AOM. Thus, even with the inclusion of AOM, the simulated Late Palaeoproterozoic atmosphere has a climatologically significant level of methane of approximately 50 ppmv.

Keywords: oxygen; methane; methanotrophy; Archaean; Proterozoic; atmospheric evolution

1. Introduction

Oxygen concentrations in the Earth's atmosphere are inferred to be less than 1 ppmv prior to *ca* 2.4 Gyr ago (Pavlov & Kasting 2002; Bekker *et al.* 2004). In such an anoxic atmosphere, photochemical models show that methane has a

* Author for correspondence (david.catling@bristol.ac.uk).

One contribution of 18 to a Discussion Meeting Issue 'Trace gas biogeochemistry and global change'.

lifetime of approximately 10^4 years and can reach levels of 10^2–10^3 ppmv, given a biogenic source of approximately 0.1–1 times present (Pavlov *et al.* 2001; Zahnle *et al.* 2006). Methane at this abundance can provide sufficient greenhouse warming to counteract an early Sun that was 25–30% fainter (Pavlov *et al.* 2000; Kasting & Howard 2006). The ultraviolet decomposition of methane in the early upper atmosphere and the accompanying escape of hydrogen to space may have also been important for irreversibly oxidizing Earth's surface environment and enabling the rise of oxygen (Catling *et al.* 2001; Claire *et al.* 2006).

Carbon and sulphur isotopes suggest that there was abundant methane in the Archaean. A global distribution of ^{12}C-enriched kerogens of 2.5–2.8 Ga age can be attributed to isotopically light CH_4, greater than 20 ppmv abundance, generated by methanogens and incorporated into methanotrophs (Hayes 1994; Hinrichs 2002; Hayes & Waldbauer 2006). Strictly speaking, this evidence only indicates that methane had to be plentiful within worldwide sediments, but independent evidence for high methane in the atmosphere is provided by mass-independent fractionation (MIF) of Archaean sedimentary sulphur isotopes (Farquhar *et al.* 2000). Abundant MIF is thought to occur only when sulphur exits the atmosphere in soluble and insoluble forms: in particular, soluble SO_4^{2-} and insoluble elemental polymerized sulphur (S_8) at different ends of the sulphur redox distribution (Pavlov & Kasting 2002). Models show that both low levels of oxygen and a sufficiently high abundance of methane are required for insoluble S_8 to be a significant photochemical product of the ancient anoxic atmosphere (Ono *et al.* 2003; Zahnle *et al.* 2006). Sufficient methane enables the photochemical reduction of sulphur-bearing gases to S_8. Thus, Zahnle *et al.* (2006) show that MIF is indirect evidence for high Archaean methane.

Evidence from biomarkers suggests that oxygenic photosynthesis arose long before the rise of atmospheric O_2 around 2.4 Gyr ago (Brocks *et al.* 2003; Summons *et al.* 2006), a puzzle that can be explained if the O_2 was efficiently scavenged by a glut of reductants in the early environment (e.g. Walker *et al.* 1983; Holland 2002; see Catling & Claire (2005) for a review). Given little O_2 and abundant CH_4 in the Archaean atmosphere, how did the atmosphere become oxygenated?

One way to understand the factors that influence the history of O_2 is through time-dependent biogeochemical box models that simulate changes in atmospheric O_2 levels as a result of redox fluxes in the Earth system. In such models, it is necessary to pay particular attention to atmospheric photochemistry in order to simulate realistic levels of O_2 or CH_4. In Catling *et al.* (2004), we presented preliminary results of a biogeochemical model where we parameterized an effective bimolecular reaction between CH_4 and O_2 with a rate constant that depended on the levels of CH_4 and O_2. We noted then that shielding of the troposphere by stratospheric ozone acts as a positive feedback on O_2 as O_2 rises (Catling *et al.* 2004). Claire *et al.* (2006) (a paper which we henceforth refer to as 'CCZ') have subsequently enhanced this model and described its sensitivities and results in considerable detail (e.g. fig. 3 in CCZ shows the effect of increasing stratospheric ozone on the effective reaction of O_2 and CH_4 from photochemical modelling). Goldblatt *et al.* (2006) present a similar model that also uses the idea of an effective bimolecular reaction between O_2 and CH_4; as in Catling *et al.* (2004), they found that ozone shielding acts as a positive feedback on the rise of O_2.

While the shielding effect of the ozone layer is important in understanding the steady-state differences between oxic and anoxic atmospheres, CCZ demonstrated that this feedback alone does not cause an abrupt rise in oxygen. Instead, we hypothesized that the biosphere provided a strong positive feedback on atmospheric O_2 by diminishing the CH_4 flux to the atmosphere relative to the O_2 flux (Zahnle *et al.* 2006). In particular, we hypothesized that the increase in oceanic sulphate (and nitrate) levels was accompanied by the increased activity of methanotrophs, which facilitated a rapid transition to an oxic atmosphere by lowering the ratio of $CH_4 : O_2$ fluxes to the atmosphere.

In this paper, we demonstrate the plausibility of this idea using our box model. Goldblatt *et al.* (2006) included aerobic methanotrophs in their model, i.e. microbes that directly use atmospheric O_2 to consume CH_4, but this has no effect on the $CH_4 : O_2$ flux ratio and so is neutral with respect to atmospheric redox. In contrast, anaerobic methanotrophs are known to use sulphate or nitrate when O_2 is unavailable in the metabolic processes of 'anaerobic oxidation of methane' (AOM). In this paper, we demonstrate how AOM was likely to have been important in determining the rapidity and magnitude of the *ca* 2.4 Gyr ago rise of O_2. We also show how AOM modulates the evolution of CH_4 levels, which has implications for Earth's climate.

2. Method: the box model and anaerobic oxidation of methane

In §2*a–c*, we describe our biogeochemical model, how AOM should influence the rise of oxygen, and how we parameterize AOM in the model.

(*a*) *Model description*

As our point of departure, we consider the atmosphere only after the advent of oxygenic photosynthesis. A full description of our biogeochemical model is given in CCZ. Here, we briefly reiterate the key equations so that modifications to take anaerobic methanotrophy into account can be appreciated.

In our model, the amount of O_2 in the atmosphere is determined by a kinetic competition between source (F_{SOURCE}) and sink (F_{SINK}) fluxes of O_2, i.e.

$$\frac{\mathrm{d}}{\mathrm{d}t}[\mathrm{O_2}] = F_{\mathrm{SOURCE}} - F_{\mathrm{SINK}} = (F_{\mathrm{B}} + F_{\mathrm{E}}) - (F_{\mathrm{V}} + F_{\mathrm{M}} + F_{\mathrm{W}}), \tag{2.1}$$

where $[O_2]$ is the total reservoir of atmospheric O_2, which we express in units of teramoles (10^{12} mol), sometimes converting to partial pressure units of bars for figures. We implement all source and sink fluxes in the model in units of Tmol O_2 yr^{-1} production or consumption. We divide F_{SOURCE} into F_{B}, the flux of oxygen due to organic carbon burial, and F_{E}, the flux of oxygen to the Earth as a whole due to hydrogen escape. The oxygen sinks F_{V} and F_{M} represent oxygen-consuming gases (i.e. H_2, H_2S, SO_2, CO, CH_4) from volcanic/hydrothermal and metamorphic/geothermal processes, respectively, while F_{W} is the oxygen sink due to oxidative weathering of continental rocks. Equation (2.1) is illustrated by summing fluxes in and out of the atmosphere–ocean–biosphere ('AOB') box in figure 1.

We ignore the gross photosynthesis–respiration cycle because this rapid, closed cycle generates no net O_2 (e.g. see Garrels & Perry (1974) or Walker (1980)). However, in order to calculate the levels of methane in the Archaean

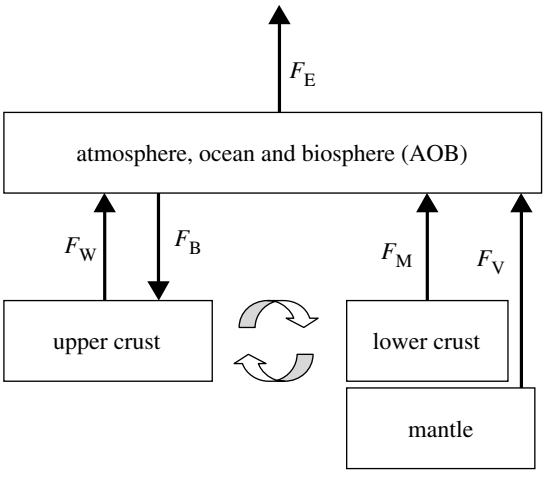

Figure 1. A schematic of the three-box model. Arrows represent fluxes of reducing material in Tmol O_2 equivalents yr^{-1}. Consequently, arrows leaving a box represent oxidizing processes. Equation (2.1) for the evolution of O_2 is obtained by subtracting incoming reductant fluxes from outgoing reductant fluxes. The unfilled arrows represent crustal mixing due to erosion, uplift and tectonics.

atmosphere, it is necessary to consider the fraction of photosynthesized carbon from gross primary productivity that gets converted to methane. The net effect of methanogenic recycling of organic carbon produced photosynthetically is found by summing the respective net reactions of oxygenic photosynthesis and methanogenesis, as follows:

$$\begin{aligned} &CO_2 + H_2O \rightarrow CH_2O + O_2 \cdots \times 2 \\ &\quad + \underline{2CH_2O \rightarrow CH_4 + CO_2} \\ &CO_2 + 2H_2O \rightarrow CH_4 + 2O_2 \end{aligned} \quad . \tag{2.2}$$

Thus, the combination of oxygenic photosynthesis and methanogenesis generates O_2 and CH_4 in the ratio of 2 : 1. Consequently, a flux of methane, ϕ_{CH_4}, to the atmosphere is accompanied by a stoichiometrically balanced flux of O_2 of $2\phi_{CH_4}$. This enables us to expand equation (2.1) to coupled time-dependent equations for the first-order evolution of atmospheric methane and oxygen

$$\frac{d}{dt}[CH_4] = \phi_{CH_4} - k_{eff}[O_2][CH_4] - k_{esc}[CH_4], \tag{2.3}$$

$$\frac{d}{dt}[O_2] = 2\phi_{CH_4} - 2k_{eff}[O_2][CH_4] - k_{esc}[CH_4] + F_B - (F_V + F_M + F_W), \tag{2.4}$$

where k_{eff} ($Tmol^{-1}\,yr^{-1}$) is the effective rate constant for a net bimolecular kinetic destruction of O_2 and CH_4. This reaction is 'effective' because it is not a real bimolecular reaction but the net result of many other reactions, starting with an attack on CH_4 by OH, the hydroxyl radical. We have numerically parameterized k_{eff} from over a thousand photochemical model runs as a function of CH_4 and O_2 levels, as described in CCZ. The constant $k_{esc} = 3.7 \times 10^{-5}$ Tmol O_2 equivalents yr^{-1} $(Tmol\ CH_4)^{-1}$ parameterizes the net photochemical destruction of methane associated with diffusion-limited hydrogen escape, $F_E = k_{esc}\,[CH_4]$. As four H atoms

escape, a CH_4 molecule is subtracted from our tally of methane in equation (2.3) by the term '$-k_{esc}$ $[CH_4]$'. The remaining carbon atom (in both anoxic and oxic atmospheres) ultimately form CO_2 by a series of photochemical reactions, which acts as a net sink for atmospheric O_2. Owing to this, one O_2 redox equivalent is subtracted from our model atmosphere in equation (2.4) in the term '$-k_{esc}$ $[CH_4]$'. However, since one molecule of methane ordinarily consumes two molecules of O_2 (the reverse of equation (2.2)), the net effect of methane-induced hydrogen escape is that the Earth gains an O_2 equivalent (Catling *et al.* 2001). Parameterizations for the following (and their corresponding sensitivities in the model) are described in CCZ and will not be repeated here: (i) evolution of the metamorphic reducing gas flux F_M as a function of crustal redox state and (ii) evolution of volcanic reducing gas flux F_V. The oxidative weathering loss is parameterized as $F_W = k_W\,[O_2]^{\beta}$, where $\beta \sim 0.4$ is a dimensionless constant (see CCZ for justification) and the constant $k_w = 0.0065\ \mathrm{Tmol}^{0.6}\,\mathrm{yr}^{-1}$ is based on the estimated modern flux, $F_W \sim 7\ \mathrm{Tmol\ O_2\ yr^{-1}}$ and the known modern concentration of oxygen, $[O_2] = 0.21\ \mathrm{bar} \times (1.78 \times 10^8\ \mathrm{Tmol\ bar^{-1}}) = 3.7 \times 10^7\ \mathrm{Tmol}$.

(*b*) *How methanotrophic feedback should influence the rise of O_2*

Microbial methanotrophy results in the oxidation of methane with O_2, sulphate or nitrate. When sufficient methane and O_2 coexist, methane-oxidizing bacteria (methanotrophs) live off the reverse of equation (2.2). But in anoxic conditions, AOM is performed by a consortium of archaea and bacteria and requires either SO_4^{2-} (e.g. Barnes & Goldberg (1976) and Reeburgh (1976) for pioneering papers or Valentine (2002) for a recent review) or NO_3^- (Raghoebarsing *et al.* 2006). The main source of oceanic SO_4^{2-} today is O_2-dependant oxidative weathering (Holland 1978; Walker & Brimblecombe 1985). The lack of $\delta^{34}S$ fractionation in Archaean marine sediments indicates low oceanic sulphate levels, which is consistent with very small fluxes of oxidative weathering (Canfield *et al.* 2000; Habicht *et al.* 2002). In terms of our model, the F_W term in equation (2.4) was very small during the Archaean. Fixation of N_2 to NH_4^+ is considered to be genetically ancient, but O_2 is required to further oxidize the ammonia to nitrate, so NH_4^+ was probably the dominant nitrogen species in Archaean oceans (Beaumont & Robert 1999; Berman-Frank *et al.* 2003).

Owing to the lack of sulphate and nitrate in the Archaean, we assumed Archaean AOM to be fully limited in the CCZ paper. Thus, all CH_4 that was likely to be made from organic carbon production was fluxed to the atmosphere. In this paper, we explore the idea that any sulphate produced as the atmosphere transits to an oxic state would allow AOM to act as a significant throttle on methane fluxes through the following net reaction for AOM, which is performed by a consortium of CH_4-oxidizing archaea and sulphate-reducing bacteria (Boetius *et al.* 2000):

$$CH_4 + SO_4^{2-} \rightarrow HS^- + HCO_3^- + H_2O. \tag{2.5}$$

In the Archaean ocean, which had abundant ferrous iron at depth, such sulphide generated by methanotrophy would be rapidly removed as iron sulphides (Walker & Brimblecombe 1985). We focus on sulphate rather than nitrate because methanotrophy with sulphate occurs at a lower redox state and

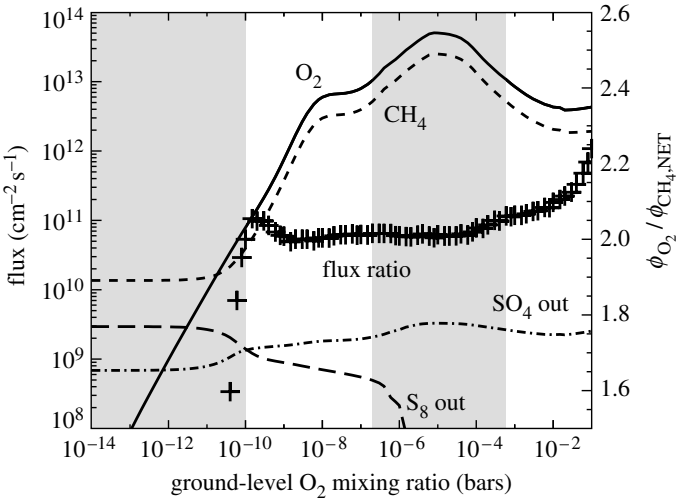

Figure 2. Major atmospheric fluxes of chemical species (in molecules $\mathrm{cm}^{-2}\,\mathrm{s}^{-1}$) as a function of the ground-level O_2 mixing ratio for a fixed CH_4 mixing ratio of 100 ppmv and fixed volcanic outgassing fluxes of sulphur gases and reducing gases (see text). Plus symbols (+) map to the right-hand ordinate axis and indicate the net ratio of the biogenic O_2 flux (ϕ_{O_2}) to CH_4 flux (ϕ_{CH_4}) as a function of the ground-level O_2 mixing ratio (equivalent to a partial pressure in bars to a 1 bar atmosphere). The shaded regions represent cases when the biogenic O_2 fluxes are either implausibly high or low.

the available evidence suggests that the nitrogen would predominantly be in the ammonium state prior to the oxic transition. Incorporation of nitrate methanotrophy and the nitrogen cycle is beyond the scope of this paper.

The key point for the evolution of the environment is that with the presence of sulphate, the reducing partner that accompanies O_2 production in equation (2.2) is changed from volatile CH_4 to involatile sulphide. Clearly, O_2 and CH_4 would no longer flux to the atmosphere in the ratio of 2 : 1 under these circumstances. We would expect this flux imbalance to help O_2 win control of the redox state of the early atmosphere. The flux imbalance should also amplify in positive feedback at the oxic transition as more sulphate is produced.

With a given outgassing flux of reduced gases, the difference between an oxic and anoxic atmosphere can result from just a few per cent increase in the ratio of $O_2 : CH_4$ fluxes, according to the calculations with the one-dimensional photochemical model that we have described in Zahnle *et al.* (2006). In this model, the $O_2 : CH_4$ flux required to support a given atmospheric composition is slightly different from 2 : 1 because atmospheric redox balance is not just between O_2 and CH_4, but modulated by rainout of photochemical oxidants and reductants, as well as the escape of hydrogen to space. Figure 2 shows results from the photochemical model for assumed sulphur outgassing fluxes of approximately 1 Tmol S yr^{-1} (a modern, high-end estimate of outgassing with $SO_2 : H_2S$ fluxes in the ratio of 10 : 1, discussed in Zahnle *et al.* 2006), a fixed methane mixing ratio of 100 ppmv, and fixed outgassing flux of H_2 (2.7 Tmol yr^{-1}) and CO (0.3 Tmol yr^{-1}). The plot shows the O_2, CH_4, SO_4^{2-} and S_8 fluxes which the photochemistry requires for a steady-state solution when the O_2 mixing ratio is set to that shown on the x-axis. The plus symbols (+) are the ratio of the O_2 and CH_4 flux curves, which map to the right-hand ordinate axis. Shaded regions in figure 2

are considered 'forbidden' because they require biogenic fluxes that are unreasonable according to arguments presented by Zahnle *et al.* (2006). Denoting O_2 and CH_4 fluxes by the symbols ϕ_{O_2} and ϕ_{CH_4}, respectively, the oxic solutions in figure 2 have slightly higher ϕ_{O_2}/ϕ_{CH_4} ratios than the anoxic solutions. The mean value of ϕ_{O_2}/ϕ_{CH_4} in the stable anoxic regime (O_2 with a mixing ratio of 1×10^{-10}–2×10^{-7}) is 2.014, while the mean ratio in the stable oxic regime (O_2 with a mixing ratio of 6×10^{-4}–0.1) is 2.11, which is an average increase of 4.8%. The flux ratio change between the most oxic anoxic atmosphere and the least oxic oxygenated atmosphere (i.e. from both sides of the forbidden, shaded region of $2\times10^{-7}<O_2<6\times10^{-4}$) is approximately 3%.

It is important to realize that for the results of our biogeochemical model, we are considering a non-steady-state, time-dependent Earth system. Consequently, one should avoid falling into a 'steady-state trap' of thinking that consumption of O_2 associated with continental sulphide weathering (which is included as a proportion of flux F_W in equation (2.4) in our model) must exactly balance any reduction of sulphate. Sulphate built up in the ocean going from the Archaean to the Proterozoic, so that the summed flux of sulphate-producing weathering plus input from photochemical sulphate rainout must have outpaced sulphide deposition in the ocean. Indeed, during the Archaean, the primary input of sulphate to the oceans would have been photochemical production in the atmosphere, as originally suggested by Walker & Brimblecombe (1985) and verified by our photochemical calculations (e.g. the sulphate rainout flux in figure 2 in the anoxic regime is approx. 0.25 Tmol S yr^{-1}). Thus, a curious subtlety is that marine microbial sulphate reduction should have exceeded the flux of sulphate from weathering in the Archaean because the sulphate at this time primarily derived from photochemical oxidation of volcanic gases. Hydrogen escape to space supported a sulphate rainout flux.

Finally, another potential subtlety is that with the wider availability of sulphate during the oxic transition, the gaseous reduced partner of O_2 may have changed from CH_4 to biogenic sulphur gases. These sulphur gases, unlike methane, are kinetically much more unstable than O_2. The photochemistry of such an atmosphere would clearly favour higher concentrations of O_2. Biogenic sulphur gases include CH_3SCH_3, OCS and CS_2. According to the review by Warneck (2000, p. 611), today's biogenic S flux of dimethyl sulphide is approximately 1.1 Tmol S yr^{-1}, which exceeds estimated volcanic sulphur fluxes ranging approximately 0.3–1 Tmol S yr^{-1}. However, the potential feedback of biogenic sulphur gases falls beyond the scope of the present paper because they are not yet implemented in either our photochemical or biogeochemical models.

(*c*) *The magnitude of AOM and its parameterization*

AOM with sulphate takes place in a narrow vertical zone in sediments called the sulphate–methane transition zone (SMTZ). Generally, in modern sediments, the sulphate–methane boundary lies at some distance (typically 0.1–4 m) below the seawater–seafloor interface. In this zone, virtually all the methane generated within marine anaerobic sediments is consumed by AOM before it can escape (Reeburgh 1996). Today, significant methane fluxes into the oceanic water column from sediments are produced only at rare places where very high methane fluxes, such as those from mud volcanoes, push the sulphate–methane boundary to within a few

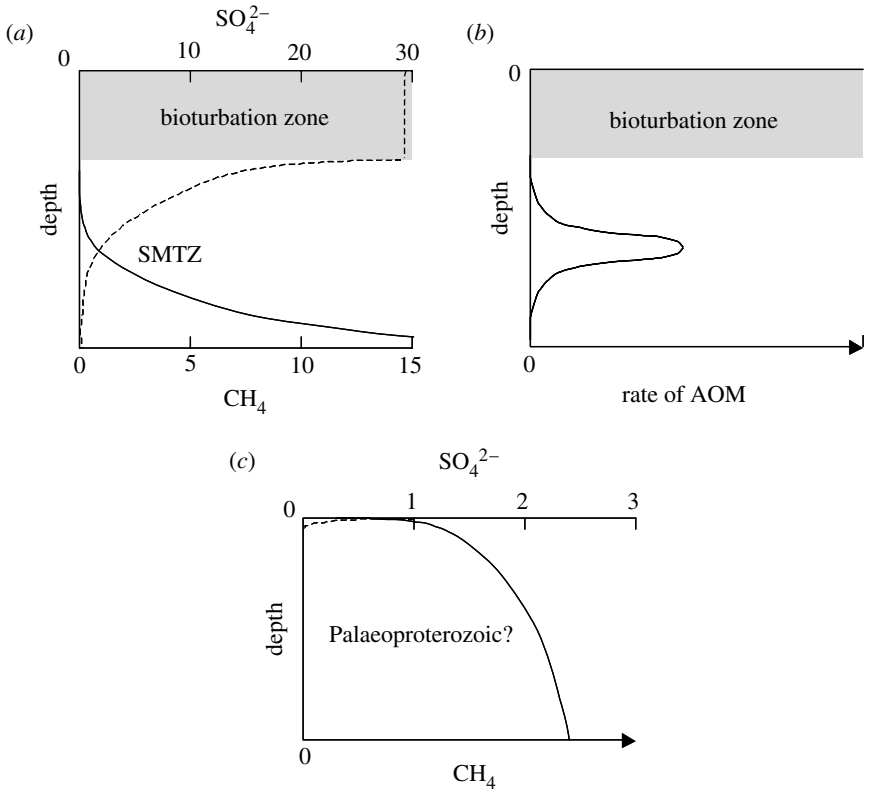

Figure 3. (*a*) A schematic showing typical profiles of methane and sulphate in modern marine sediments, where SMTZ is the sulphate–methane transition zone. Solid line, methane concentration in pore waters (mM); dashed line, sulphate concentration in pore waters (mM). Depth is relative. (*b*) A schematic showing the profile of AOM rate that corresponds to (*a*). (*c*) A schematic of relative methane concentration (solid line) and sulphate concentration (dashed line in millimolar) for the Palaeoproterozoic.

centimetres or less of the seafloor (Luff & Wallmann 2003). Consequently, today's oceans are estimated to be a relatively minor source of methane whereas land-based freshwater wetlands are relatively significant owing to their lack of sulphate.

In the Archaean and during the oxic transition, the vertical redox profile of marine sediments is likely to have been markedly different from today. Figure 3*a* shows a schematic of the modern profile of sulphate and methane in marine sediments. Modern seawater contains around 29 mM of sulphate, which is often well mixed by fauna into a bioturbation zone at the top of sediments. Below this bioturbation zone, the sulphate concentration starts to decline due to microbial sulphate reduction. Typically, methane concentrations are found to increase below the depth where sulphate concentrations fall below approximately 0.5–5 mM (Iversen & Jorgensen 1985; Whiticar 2002). The crossover depth, where sulphate and methane concentrations are small and roughly similar, is generally close to where the peak rate of AOM occurs (figure 3*b*; Devol 1983; Haese *et al.* 2003). In Archaean sediments, there would be no bioturbation zone. Moreover, Archaean oceanic sulphate concentrations were less than 0.2 mM (Habicht *et al.* 2002), so methane

would be abundant in sediments all the way to the seafloor, where methane would flux out. During the rise of oxygen, the SMTZ would be a narrow interface just below the seafloor (figure 3*c*).

The flux of methane consumed in modern marine sediments per unit area, f_{AOM}, can be estimated from empirical data as

$$f_{\mathrm{AOM}} \sim Hr_{\mathrm{AOM}}. \tag{2.6}$$

Generally, there is a bell-shaped curve with depth of the AOM rate (figure 3*b*), and in equation (2.6), H is its characteristic half-width. The rate of AOM, r_{AOM}, is given by

$$r_{\mathrm{AOM}} = K_{\mathrm{AOM}} C_{\mathrm{SO_4}} C_{\mathrm{CH_4}}, \tag{2.7}$$

where K_{AOM} is an empirical kinetic rate constant, and $C_{\mathrm{SO_4}}$ and $C_{\mathrm{CH_4}}$ are the concentrations within the SMTZ (Luff & Wallmann 2003; Wallmann *et al.* 2006). K_{AOM} depends on the abundance and activity of the AOM microbial community (Wallmann *et al.* 2006) but a reasonable average value is $K_{\mathrm{AOM}} \sim 8\ \mathrm{mM}^{-1}\ \mathrm{yr}^{-1} = 8\ \mathrm{mol}^{-1}\ \mathrm{m}^3\ \mathrm{yr}^{-1}$ (Van Cappellen & Wang 1996). Typical concentrations at the sulphate–methane transition are $C_{\mathrm{SO_4}} \sim 3\ \mathrm{mM} = 3\ \mathrm{mol\ m}^{-3}$, $C_{\mathrm{CH_4}} \sim 1\ \mathrm{mM} = 1\ \mathrm{mol\ m}^{-3}$ and $H = 0.04$ m (Devol 1983; Iversen & Jorgensen 1985; Haese *et al.* 2003), giving an estimate of $f_{\mathrm{AOM}} = (0.04\ \mathrm{m})(8\ \mathrm{mol}^{-1}\ \mathrm{m}^3\ \mathrm{yr}^{-1})(3\ \mathrm{mol\ m}^{-3})(1\ \mathrm{mol\ m}^{-3}) \sim 1\ \mathrm{mol\ CH_4\ m}^{-2}\ \mathrm{yr}^{-1}$. This value is consistent with the observation that a typical shelf sediment has a total C mineralization of about 10 mol C $\mathrm{m}^{-2}\ \mathrm{yr}^{-1}$, of which about 10% is due to methanogenesis, giving approximately 1 mol $\mathrm{CH_4\ m}^{-2}\ \mathrm{yr}^{-1}$ (Canfield 1991; Middelburg *et al.* 1997). Most organic matter accumulates in coastal sediments or ocean margin sediments that represent approximately 7 and 9% of the ocean area, respectively (Middelburg *et al.* 1997), with the former probably more important for methane generation. Given that the total ocean area is $1.8 \times 10^{14}\ \mathrm{m}^2$, if roughly 10% of it generated an estimated 1 mol $\mathrm{CH_4\ m}^{-2}\ \mathrm{yr}^{-1}$, the global amount of methane consumed today by marine AOM would be $(0.1)(1.8 \times 10^{14}\ \mathrm{m}^2)(1\ \mathrm{mol\ m}^{-2}\ \mathrm{yr}^{-1}) \sim 18\ \mathrm{Tmol\ CH_4\ yr}^{-1}$. This value is broadly consistent with an independent estimate of the global AOM rate from Hinrichs & Boetius (2002). They estimate mean AOM rates of 0.37, 0.22, 0.22 and 0.073 mol $\mathrm{m}^{-2}\ \mathrm{yr}^{-1}$, for inner shelf, outer shelf, inner margin and outer margin regions, respectively, and derive a global flux of approximately 24 Tmol $\mathrm{CH_4\ yr}^{-1}$ when high flux seepage areas are also added. Thus, a potentially large flux of methane of a few tens of Tmol $\mathrm{CH_4\ yr}^{-1}$ magnitude apparently never escapes from the marine sediments; this flux can be compared with the estimated total global flux of methane from all sources that actually reaches the modern atmosphere, which ranges from 31 to 38 Tmol $\mathrm{CH_4\ yr}^{-1}$ (Prather *et al.* 2001).

The estimate of a few tens of Tmol $\mathrm{CH_4\ yr}^{-1}$ from modern AOM rates may underestimate the amount of methane that was generated in the largely anoxic Archaean after the advent of oxygenic photosynthesis. Methane is produced from organic carbon that would otherwise be buried or used for reduction of local oxygen carriers such as sulphate; in anaerobic sediments, organic carbon reduces sulphate directly, i.e. $\mathrm{SO_4^{2-} + 2\ CH_2O = H_2S + 2\ HCO_3^-}$. The average ratio of the AOM rate to the rate of sulphate reduction by organic matter in modern continental margins is estimated to be approximately 30% (Hinrichs & Boetius 2002). Taking the modern rate of methanogenesis as approximately 24 Tmol $\mathrm{CH_4\ yr}^{-1}$, in the absence of sulphate, the potential rate of

methanogenesis could have been approximately 100 Tmol $CH_4\,yr^{-1}$. We adopt this value as a baseline estimate for the global flux of methane from all sediments, ϕ_{CH_4}, in our biogeochemical model for the Archaean and Early Proterozoic, as expressed in equations (2.3) and (2.4). In §3, we describe the sensitivity of the model to this parameter. When methane fluxes are high and sulphate levels low, data from modern environments suggest that almost all sulphate couples to the AOM (Aharon & Fu 2000; Boetius *et al.* 2000). Thus, in the Archaean and the Early Proterozoic, as a first-order approximation, we assume that AOM was the major process coupled with sulphate reduction, as argued by Hinrichs (2002) and Hinrichs & Boetius (2002).

We have previously suggested that the Archaean ocean could have provided a large flux of methane approximately 10^2 Tmol $CH_4\,yr^{-1}$ to the atmosphere owing to the lack of global reservoirs of sulphate and oxygen (Claire *et al.* 2006). How would the methane flux vary in time when sulphate levels increased? During the rise of oxygen, methane would be consumed at the seafloor in proportion to small amounts of increasing sulphate, according to equation (2.6). But once sulphate concentrations exceeded approximately 5 mM, the SMTZ would be pushed far below the seafloor into sediments, as it generally is today. At this point, virtually all the methane would be consumed by AOM and further increases in sulphate would not be expected to make any significant difference to the methane flux that escapes from sediments. Thus, the characteristic shape of the response of total AOM to sulphate may look like that schematically shown in figure 4. Proterozoic levels of sulphate after the rise of O_2 are constrained from sulphur isotopes to have been between 1.5 and 4.5 mM for *ca* 1 Gyr (Shen *et al.* 2003; Kah *et al.* 2004). Our proposed shape of the high sulphate end of the curve in figure 4 is probably relevant only to the Late Proterozoic 'second rise of O_2' at *ca* 0.6 Gyr ago (Fike *et al.* 2006; Canfield *et al.* 2007), because once sulphate levels exceeded approximately 5 mM, there is potential for rapid growth in oceanic sulphate and atmospheric O_2 levels. In this paper, we leave the second rise of O_2 to future work and restrict ourselves to examining the *ca* 2.4 Gyr ago Palaeoproterozoic oxic transition.

To a first approximation, the global flux of CH_4 to the atmosphere is modulated by subtracting the flux of CH_4 consumed by anaerobic methanotrophy. Thus, we modify equation (2.3) as follows:

$$\frac{\mathrm{d}}{\mathrm{d}t}[CH_4] = (\phi_{CH_4} - F_{AOM}) - k_{eff}[O_2][CH_4] - k_{esc}[CH_4], \tag{2.8}$$

where F_{AOM} is the global AOM in Tmol O_2 equivalents yr^{-1}, which is related to sulphate availability and hence the amount of O_2 in the atmosphere. To relate average oceanic sulphate concentrations to atmospheric O_2 levels, we use a semi-empirical approximation. Kah *et al.* (2004) derive a curve for the evolution of Precambrian oceanic sulphate levels based on sulphur isotope data and carbonate-associated sulphate from ancient sediments. For the period of interest, the Late Archaean to Paleoproterozoic, marine sulphate concentrations range from less than 0.2 mM before 2.2 Ga, to approximately 0.7 mM at 1.7 Ga and 1.9–2.0 mM at 1.5 Ga. A power-law parameterization that crudely captures this behaviour for the Archaean and Palaeoproterozoic is

$$C_{SO_4} = k_{SO_4}[O_2]^{0.4}, \tag{2.9}$$

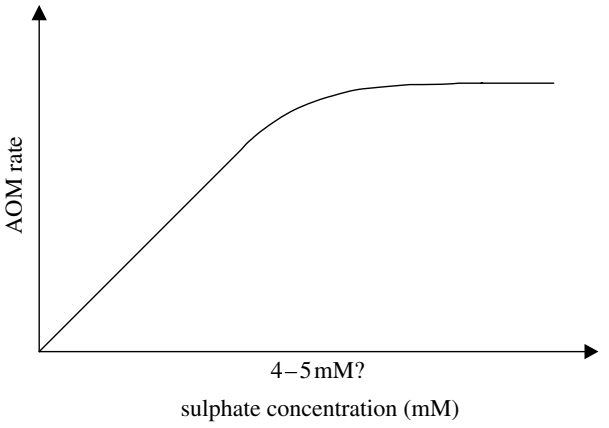

Figure 4. A schematic of the global rate of consumption of methane from AOM as the oceanic sulphate concentration increases.

where $k_{SO_4} \sim 0.003$ mM Tmol$^{-0.4}$; $[O_2]$ is in Tmol; and C_{SO_4} is in mM. Here, $[O_2]$ is consistent with estimates and models for the Archaean and Late Palaeoproterozoic (Catling & Claire 2005; Canfield 2005), but we note that there is considerable uncertainty in this regard.

To relate ocean sulphate concentrations to the global rate of AOM, we consider a simple AOM model. AOM can be modelled given methane and sulphate profiles, along with sediment porosity (Martens & Berner 1977). A common method of estimating AOM rates is to assume that all AOM takes place in an infinitely thin layer at the depth where sulphate concentrations vanish (Haese *et al.* 2003; Jorgensen *et al.* 2004). In the simplest possible model, we ignore advection through fractures and faults, since most marine sediments are dominated by diffusion. Thus, the rate of methane consumption must be balanced by the downward diffusion of sulphate (J, e.g. in mol m^{-2} yr^{-1}) into the seafloor by Fick's first law (Berner 1980)

$$J_{SO_4} = -\phi D_s \frac{\partial C}{\partial x}\bigg|_{AOM}, \tag{2.10}$$

where ϕ is the sediment porosity; C is the sulphate concentration in mol m^{-3} (numerically equivalent to millimolar); x is the depth in the sediment; and D_s is the diffusion coefficient in marine sediments. Porosity ϕ varies from 1.0 at the seafloor–water interface to smaller values with depth due to sediment compaction; for our model, where we are concerned with shallow penetration depths of low sulphate oceans, we assume a value of $\phi \sim 0.8$. The sediment diffusion coefficient for sulphate depends on temperature and porosity. Taking a typical sediment temperature of approximately 4°C, we use $D_s \sim 3 \times 10^{-10}$ m^2 s^{-1} (Iversen & Jorgensen 1993). The concentration gradient of sulphate is $\partial C/\partial x$, which goes from the seafloor to the depth x_{AOM}, of the maximum rate of AOM where $C \to 0$. Sulphate reduction and oxidation of methane at the sulphate–methane transition is arguably the most important factor for the depth of the sulphate profile and its often quasi-linear shape when AOM dominates sulphate reduction (Jorgensen *et al.* 2004). Owing to this, we adopt a simple linear approximation to equation (2.10)

$$J_{AOM} = -J_{SO_4} = \phi D_s \frac{\partial C}{\partial x}\bigg|_{AOM} = \phi D_s \frac{C_{SO_4}}{x_{AOM}}. \tag{2.11}$$

This area flux is multiplied by area A, which we take as 10% of the ocean area, to give an estimated global flux F_{AOM}, of AOM. We note that coastal and shelf sediment area A should depend on the amount of continental landmass. The time evolution of the growth of the continents remains a controversial, open field of inquiry but most models predict that at least 70% of the current continental volume was in place by 2 Ga (Patchett & Arndt 1986; Rogers & Santosh 2004, p. 48), which is close to the time of interest for this paper.

The AOM flux in equation (2.11) depends on sulphate concentrations and the depth of the sulphate–methane transition, i.e. x_{AOM}. In modern sediments, there is commonly a bioturbation zone that mixes sulphate downwards uniformly (figure 3*a*), and in this case, x_{AOM} is the depth beneath the base of the bioturbation zone rather than below the sediment–water interface. Defined in this way, x_{AOM} varies from a few centimetres depth in shallow coastal sediments to metres depth on the continental slope (Borowski *et al.* 1999; Kruger *et al.* 2005). In the modern ocean, x_{AOM} appears to be a function of organic content of sediments and methane supply (Borowski *et al.* 1996). Hence, x_{AOM} is a few centimetres depth around Black Sea mud volcanoes (Wallmann *et al.* 2006) when compared with many metres depth in oceanic sediments in regions of low methane flux. Since we are concerned with an anoxic, low sulphate ocean in the Archaean that progresses to an ocean with a few millimolar sulphate in the Proterozoic, we note that for some globally averaged methane flux from sediments, at low sulphate levels, x_{AOM} must primarily depend on sulphate concentrations in the overlying water to a first approximation. For example, in lakes with anoxic bottom waters and sulphate approximately 2–5 mM, x_{AOM} depths are very close to the water–sediment interface (Ingvorsen & Brock 1982), while freshwater stratified lakes with less than 0.01 mM sulphate essentially have negligible AOM (Reeburgh & Heggie 1977). Consequently, we parameterize the globally averaged depth of maximum AOM, as follows:

$$x_{\mathrm{AOM}} = k_{\mathrm{SMTZ}} C_{\mathrm{SO_4}}^{\alpha}, \tag{2.12}$$

where k_{SMTZ} and α are constants. The connection of the average depth of AOM to sulphate concentrations in marine sediments has received little detailed investigation because modern seawater sulphate concentrations are uniform at 29 mM. Thus, the choice of k_{SMTZ} and α is arbitrary; consequently, we investigate the sensitivity of the model to these parameters when considering the results. We choose baseline values of $k_{\mathrm{SMTZ}}=0.1$ and $\alpha=0.4$, for which x_{AOM} varies from approximately 1–15 cm over sulphate concentrations of approximately 0.005–3 mM. Taking equation (2.12) and inserting into equation (2.11) gives the parameterization for the global AOM flux for the Archaean to the Proterozoic, as follows:

$$F_{\mathrm{AOM}} = A\phi D_{\mathrm{s}} \frac{C_{\mathrm{SO_4}}^{(1-\alpha)}}{k_{\mathrm{SMTZ}}}. \tag{2.13}$$

A full general treatment of the effect of AOM on the rise of O_2 would involve isolating the ocean from the atmosphere in our box model and examining all sulphur fluxes in and out of the ocean constrained by the isotopic record, i.e. integrating a complete sulphur cycle to our biogeochemical model. However, even adding one process such as AOM introduces two new free parameters,

therefore a full model would obviously introduce many more. For present purposes, our rough approximations are sufficient to demonstrate the potential of AOM feedback to affect the history of O_2 and CH_4.

3. Results and discussion

We present the results of two numerical experiments that both perform a modulation of the methane flux according to equation (2.8). The first uses a simplistic approximation without the AOM model developed above. The second makes use of the AOM model captured in equation (2.13).

(*a*) *Method 1: simple modulation of the CH_4 flux*

For the first numerical experiment, we modulate the methane flux according to equation (2.8) with a factor that depends directly on oxidative weathering. Let us take the estimate that 45% of the oxidative weathering flux is used to mobilize sulphate (Holland 2002) and assume that the sulphate washed to the ocean by rivers is immediately available for methanotrophy. Thus, we take $F_{\mathrm{AOM}} = 0.45F_{\mathrm{W}}$ where F_{W} is the oxidative weathering flux, which is parameterized as a function of atmospheric O_2 levels as described in §2. The advantage of this crude experiment is that it allows us to investigate the potential effects of any positive feedback and understand them algebraically.

Figure 5*a* shows the results of including this AOM feedback when compared with the reference model of CCZ with $\phi_{\mathrm{CH_4}} = 100\ \mathrm{Tmol\ CH_4\ yr^{-1}}$, as discussed in §2*c*. Figure 5*b* shows the corresponding AOM fluxes and seawater sulphate concentrations. O_2 rises more rapidly when AOM is included and to a level about an order of magnitude higher than that without AOM. Surprisingly, methane 're-rises' faster after the oxic transition and to a higher value in this new scheme, despite the consumption of methane by AOM. Algebraic analysis helps explain this apparently counter-intuitive behaviour of methane. We can solve equation (2.3) in the steady state ($\mathrm{d}[\mathrm{CH_4}]/\mathrm{d}t = 0$) by assuming that the hydrogen escape term is a minor term after the rise of O_2 (i.e. $F_{\mathrm{E}} = k_{\mathrm{esc}}[\mathrm{CH_4}] \to 0$)

$$\mathrm{CH_4}\Big|_{\mathrm{Oxic}} = \frac{\phi_{\mathrm{CH_4}} - F_{\mathrm{AOM}}}{k_{\mathrm{eff}}[\mathrm{O_2}]}. \tag{3.1}$$

The effective rate constant, k_{eff}, has a nonlinear dependence on CH_4 and O_2 levels, particularly below an O_2 level of 10^{-6} bar and for CH_4 levels more than 10^{-4} bar (see fig. 3 in the CCZ paper). However, in the region $\mathrm{O_2} > 10^{-6}$ bar and $\mathrm{CH_4} < 10^{-4}$ bar, the dependence of k_{eff} on $[\mathrm{O_2}]$ is approximately linear on a log–log plot so that a least-squares fit provides a power-law relationship, as follows (with correlation coefficient $R^2 = 0.994$):

$$k_{\mathrm{eff}}(\mathrm{O_2}) = 1.8368[\mathrm{O_2}]^{-1.2448}, \tag{3.2}$$

where $[\mathrm{O_2}]$ is the global amount of atmospheric O_2 in Tmol. Equation (3.2) is applicable for $[\mathrm{O_2}]$ amounts in the atmosphere greater than approximately 100 Tmol, where this amount of oxygen is equivalent to a partial pressure of

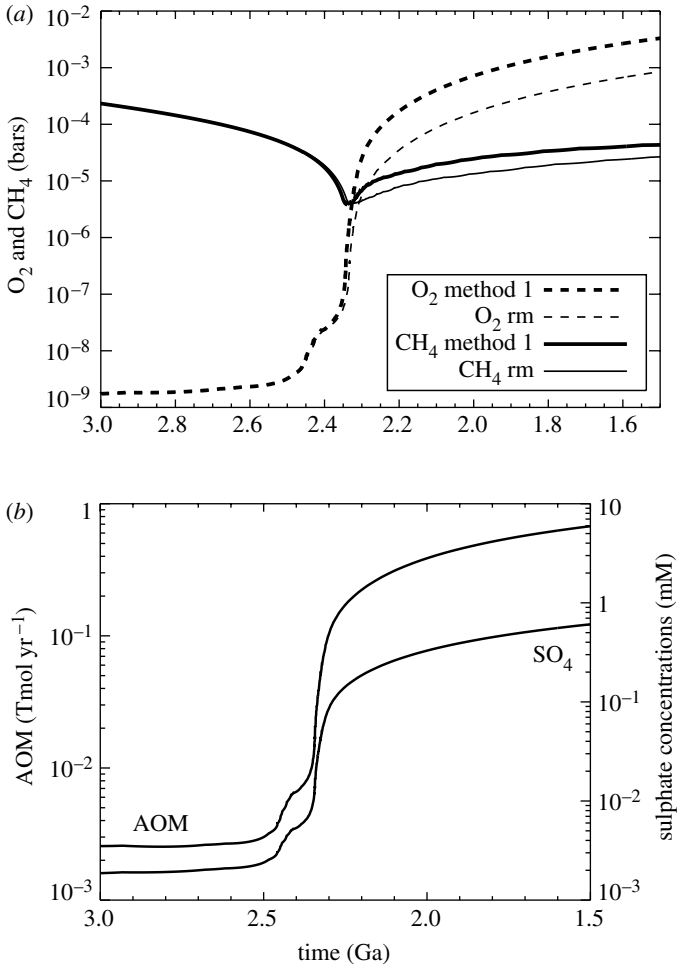

Figure 5. (*a*) A comparison of the evolution of O_2 and CH_4 from the biogeochemical model with and without the inclusion of AOM using 'method 1' (see text). The model with AOM is labelled method 1 and the model without AOM is the reference model of Claire *et al.* (2006), labelled 'rm'. (*b*) Corresponding plot of simulated seawater sulphate concentrations AOM rates versus time for method 1.

approximately 10^{-6} bar in a 1 bar atmosphere. Substituting equation (3.2) into equation (3.1) gives

$$[\mathrm{CH_4}]\Big|_{\mathrm{Oxic}} = \frac{\phi_{\mathrm{CH_4}} - F_{\mathrm{AOM}}}{k_{\mathrm{eff}}[\mathrm{O_2}]} = 0.544(\phi_{\mathrm{CH_4}} - F_{\mathrm{AOM}})[\mathrm{O_2}]^{0.2448}. \tag{3.3}$$

In the absence of anaerobic methanotrophs, $F_{\mathrm{AOM}}=0$, hence post-transition CH_4 levels in the reference model are a monotonically increasing function of O_2. In other words, for a given methane flux, the effective rate constant for the oxidation of methane by oxygen in the atmosphere decreases with increasing $[O_2]$ according to equation (3.2), an effect that can be traced to the influence of a thickening stratospheric ozone layer (Catling *et al.* 2004; Claire *et al.* 2006; Goldblatt *et al.* 2006). If we substitute $F_{\mathrm{AOM}}=0.45F_{\mathrm{W}}=0.45k_{\mathrm{W}}[\mathrm{O_2}]^{\beta}$ with $\beta=0.4$ and $k_{\mathrm{W}}=0.006$

into equation (3.3), we obtain

$$[\mathrm{CH_4}]\Big|_{\mathrm{Oxic}} = \phi_{\mathrm{CH_4}} 0.544 \left([\mathrm{O_2}]^{0.2448} - \frac{0.45 k_{\mathrm{W}}}{\phi_{\mathrm{CH_4}}} [\mathrm{O_2}]^{0.6448} \right)$$
$$= 108.8([\mathrm{O_2}]^{0.2448} - 1.35 \times 10^{-5} [\mathrm{O_2}]^{0.6448}). \tag{3.4}$$

In evaluating the numerical constant, we take the gross production flux of methane $\phi_{\mathrm{CH_4}}$, as a 200 Tmol $\mathrm{O_2\,yr^{-1}}$ sink, equivalent to a worldwide production of 100 Tmol $\mathrm{CH_4\,yr^{-1}}$ in all Archaean–Proterozoic anaerobic sediments, as discussed earlier. Comparing the two terms on the right-hand side reveals that the first term is a factor of 10^2–10^3 higher over the range of $\mathrm{O_2}$ values considered for the Proterozoic after the oxic transition. Thus, in the methanotroph-modified world, $\mathrm{CH_4}$ levels increase at higher $\mathrm{O_2}$ levels in the Palaeoproterozoic despite the lower $\mathrm{CH_4}$ flux; this is primarily a result of atmospheric chemistry as captured by k_{eff}. Overall, the results of our numerical experiment are consistent with the idea that $\mathrm{CH_4}$ continued to be a significant greenhouse gas in the Proterozoic, albeit at a lower concentration than in the Archaean (Pavlov *et al.* 2003; Claire *et al.* 2006; Zahnle *et al.* 2006).

(*b*) *Method 2: modulation of CH_4 fluxes by parameterized AOM*

In our second numerical experiment, we modulate the methane flux to the atmosphere in equation (2.8) based on relationships given in §3*a* where sulphate diffusion into sediments balances the flux of methane consumed by AOM.

Figure 6*a* shows the results of using the parameterizations described by equations (2.11) and (2.12) ('method 2'), compared to the results presented in §3*a*. The $\mathrm{O_2}$ and $\mathrm{CH_4}$ curves are qualitatively similar in shape and slope, although the curves generated from computing F_{AOM} using method 2 hasten the time of oxic transition by *ca* 0.1 Gyr. Figure 6*b* shows the two curves referenced to the oxic transition; with method 2, $\mathrm{O_2}$ rises from less than 10^{-6} to 10^{-4} bar in *ca* 0.05 Gyr, about twice as rapidly as 'method 1'.

The effect on the timing of the transition can be understood with algebra. In CCZ, we discussed the timing of the oxic transition in terms of the fluxes of organic burial (F_{B}) versus the flux of $\mathrm{O_2}$-consuming species from volcanism/hydrothermal (F_{V}) plus metamorphism/geothermal reductants (F_{M}), following an argument originally advanced by Walker *et al.* (1983). Essentially, the oxic transition occurs at the point when the $\mathrm{O_2}$ produced by the organic burial flux, F_{B}, exceeds the sum of the reductant fluxes, $F_{\mathrm{V}} + F_{\mathrm{M}}$. Consequently, in CCZ, we defined an oxygenation parameter K_{OXY}, based on kinetically active reduced gases in the ground-level atmosphere and reduced cations in the ocean

$$K_{\mathrm{OXY}} = \frac{F_{\mathrm{SOURCE}}}{F_{\mathrm{REDUCED\ SINKS}}} \sim \frac{F_{\mathrm{B}}}{F_{\mathrm{V}} + F_{\mathrm{M}}}. \tag{3.5}$$

We define the atmosphere as oxygenated when $K_{\mathrm{OXY}} > 1$. If we include methanotrophy, it can impact K_{OXY} and hence the timing of the oxic transition in the following manner. An approximate steady-state solution for the evolution of $\mathrm{CH_4}$ at the time of the oxic transition can be found by setting the hydrogen escape term,

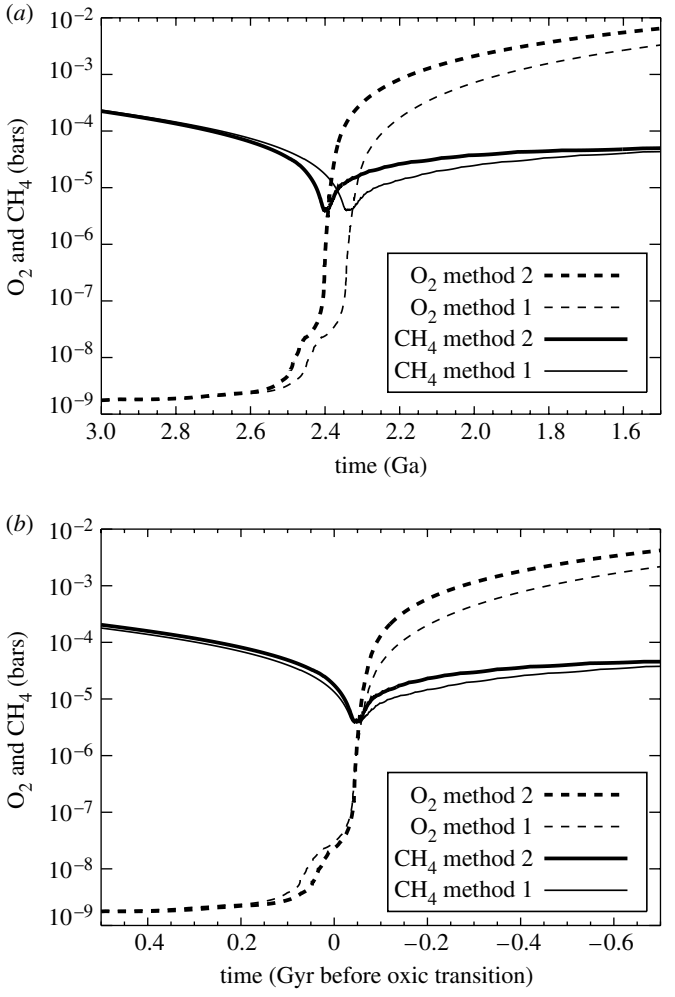

Figure 6. (*a*) A comparison of the evolution of O_2 and CH_4 in the model using method 1 and 'method 2' (see text). (*b*) The plots for each model run where the time axis has been referenced to the time (equal to 0) of the oxic transition.

$F_E = k_{esc}\,[CH_4]$, to zero in equation (2.3) to obtain

$$\phi_{CH_4}|_{trans} \simeq F_{AOM} + k_{eff}[O_2][CH_4]. \tag{3.6}$$

Taking $F_E = 0$ and substituting twice equation (3.6) into equation (2.4) yields an equation for the evolution of O_2 at the time of the oxic transition

$$\frac{d}{dt}[O_2]\Big|_{trans} = 2F_{AOM} + F_B - (F_V + F_M + F_W). \tag{3.7}$$

The balance on the right-hand side of equation (3.7) provides an expanded version of the oxygenation parameter (K^*_{OXY}) that includes the AOM flux, F_{AOM}

$$K^*_{OXY} \sim \frac{F_B + 2F_{AOM}}{F_V + F_M + F_W}. \tag{3.8}$$

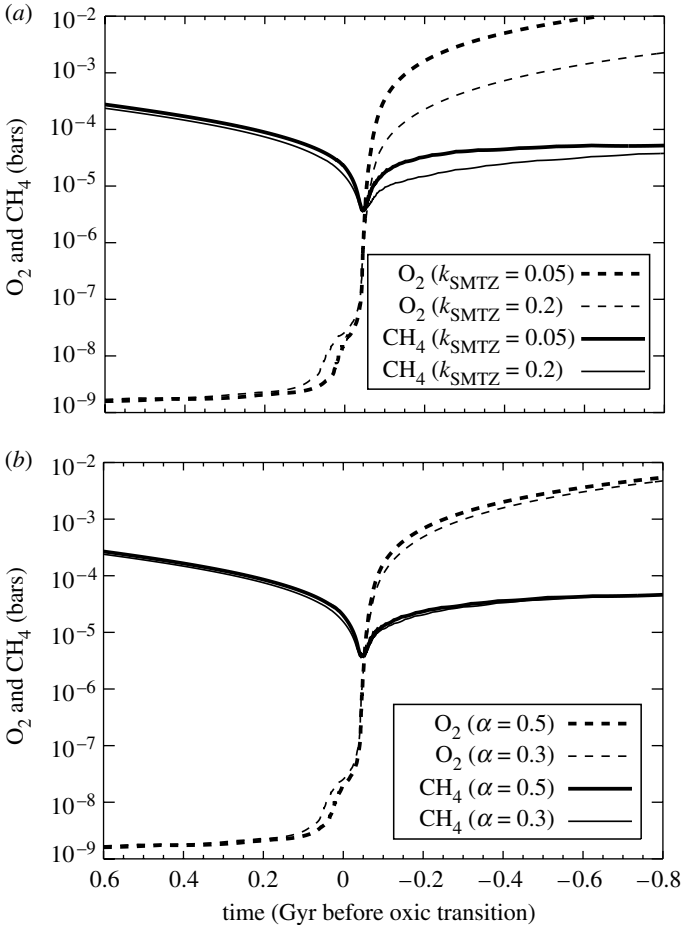

Figure 7. (*a*) Sensitivity of the model to changes in parameter k_{SMTZ}. (*b*) Sensitivity of the model to changes in parameter α.

Method 1 used $F_{\mathrm{AOM}}=0.45F_{\mathrm{W}}$ so that $2F_{\mathrm{AOM}}\sim F_{\mathrm{W}}$ and K^{*}_{OXY} is approximately equal to K_{OXY} in the reference model. Thus, by coincidence, the timing of the oxic transition was essentially the same. In method 2, the numerical values of F_{AOM} were approximately equal in magnitude to F_{W} at the time of the oxic transition so that K^{*}_{OXY} reached unity somewhat before K^{*}_{OXY} of method 1.

Equation (2.12), which forms part of the parameterization of AOM, has two free parameters (k_{SMTZ} and α) and we can examine how the model responds to their choice. For the comparison between different parameter choices, we ignore the effect on the timing of the oxic transition because this actually lacks real significance: the timing of this transition in the model is primarily determined by the choice of the parameterization of F_{V} and F_{M}, as described in the CCK paper, and so it is necessarily a tuned parameter. Instead, we reference the time to the oxic transition when $K^{*}_{\mathrm{OXY}}=1$. In this manner, figure 7 shows the model sensitivities to changing k_{SMTZ} and α from our reference values of 0.1 and 0.4. Figure 7*a* shows that decreasing k_{SMTZ} sharpens the rate of the oxic transition

and increases the post-oxic atmospheric O_2 and CH_4 concentrations. Effectively, when k_{SMTZ} is decreased, k_{SMTZ} AOM rates increase. In contrast, figure 7*b* shows that the model is relatively insensitive to the choice of α.

Finally, the qualitative results of the model are insensitive to the exact value chosen for the global methane flux generated in all sediments, ϕ_{CH_4}, which we have nominally taken as 100 Tmol CH_4 yr^{-1} (see §2*c*). The main effect of changing ϕ_{CH_4} is to alter the level of the minor gas (O_2 or CH_4) in the anoxic or oxic worlds. In the case of lower ϕ_{CH_4}, O_2 is lower in the Archaean, while CH_4 is proportionately lower in the Proterozoic, as predicted by equation (3.1).

4. Conclusions

Empirical data show that a significant flux of CH_4 is consumed by AOM in modern marine sediments before the methane even reaches the seafloor. This flux is estimated as roughly 20 Tmol CH_4 yr^{-1} (§2*c*). Consequently, a large amount of biogenic methane never reaches the modern atmosphere. However, in the Archaean ocean with less than 0.2 mM sulphate, AOM and other forms of sulphate reduction would have been limited by the lack of oxidized substrate so that methanogenesis would arguably have dominated recycling of organic carbon. In this case, a very large flux of methane approximately 100 Tmol CH_4 yr^{-1} produced in anaerobic marine sediments could have fluxed out to the atmosphere. For some perspective, this flux is only 1% of modern net primary productivity approximately 10^4 Tmol C yr^{-1}.

Approaching, during and after the oxic transition, the $\delta^{34}S$ record in marine sediments suggests that the flux of sulphate to the oceans from continental oxidative weathering increased, consistent with the physical expectation that dissolved oxygen in rainwater and rivers would oxidize continental pyrite to sulphate (Habicht *et al.* 2002). We have shown how methanotrophy can act to diminish methane fluxes to the Late Archaean atmosphere in the presence of increasing oceanic sulphate. This feedback means that gas fluxes to the atmosphere of O_2 and CH_4 increase slightly from the 2 : 1 ratio predicted from equation (2.2) because the reducing power of methane is converted to involatile sulphide.

When we include a simple AOM feedback in our model, O_2 rises more rapidly and to a higher value than in the model without the AOM feedback. The time-scale for the oxic transition is shortened, while O_2 rises to a level of a few $\times 10^{-3}$ bar (a few per cent of present levels) by 2.1 Gyr ago instead of approximately 10^{-4} bar in the reference model. Methane also re-rises faster and to a value of approximately 50 ppmv by the end of the Palaeoproterozoic, which is higher than that in the model without AOM feedback. At first sight, obtaining a higher level of Proterozoic methane when AOM is included in the model seems counter-intuitive because AOM diminishes the CH_4 flux to the atmosphere. However, the dominant effect of AOM is to enable O_2 to rise more rapidly to a higher level; consequently, methane levels also rise more rapidly to a higher level because they are enhanced more strongly by the effect of increased shielding effect of the stratospheric ozone layer than decreased by the lowering of the methane flux by AOM. We note that the effect of the nonlinear dependence of AOM at higher O_2 levels (figure 4) is not included in the model and may have been important for the Late Proterozoic second rise of O_2 *ca* 0.6 Gyr ago.

We have shown previously that CH_4 levels should have collapsed in the Early Proterozoic before there was sufficient atmospheric O_2 to be detectable through conventional geologic indicators such as red beds and palaeosols (Zahnle *et al.* 2006). The counter-intuitive twist that methanotrophy allows CH_4 to re-rise after the oxic transition to higher levels in the Proterozoic is relevant to the Proterozoic climate. Stable, relatively high levels of methane in the Proterozoic may help account for a prolonged period exceeding 1 Gyr where there is no reliable evidence for glaciation (Eyles 1993). Moderately abundant methane could have provided a greenhouse effect that compensated for a fainter Proterozoic Sun (Pavlov *et al.* 2003). The total oxidation of the Earth from the slow leak of hydrogen via methane-induced hydrogen escape may also be important when integrated over more than 1 Gyr of the Proterozoic, as mentioned in Catling & Claire (2005).

Finally, our computational experiments provide motivation for laboratory experiments and fieldwork. Clearly, more field data would constrain controls on AOM in sediments and the globally averaged magnitude of AOM, while, in principle, an O_2-free chamber in the laboratory could simulate the response of AOM in marine sediments to increasing levels of seawater sulphate.

M.W.C. acknowledges support of NSF IGERT award DGE09870713 awarded to the University of Washington's Astrobiology Program and NASA Exobiology Program grant NNG05GGQ25G awarded to D.C.C. at the University of Washington. D.C.C. also acknowledges the support of a European Union Marie Curie Chair award. K.J.Z. acknowledges support from NASA's Exobiology Program. The authors thank two anonymous referees whose comments much improved the manuscript.

References

Aharon, P. & Fu, B. S. 2000 Microbial sulfate reduction rates and sulfur and oxygen isotope fractionations at oil and gas seeps in deepwater Gulf of Mexico. *Geochim. Cosmochim. Acta* **64**, 233–246. (doi:10.1016/S0016-7037(99)00292-6)

Barnes, R. O. & Goldberg, E. D. 1976 Methane production and consumption in anoxic marine-sediments. *Geology* **4**, 297–300. (doi:10.1130/0091-7613(1976)4<297:MPACIA>2.0.CO;2)

Beaumont, V. & Robert, F. 1999 Nitrogen isotope ratios of kerogens in Precambrian cherts: a record of the evolution of atmosphere chemistry? *Precambrian Res.* **96**, 63–82. (doi:10.1016/S0301-9268(99)00005-4)

Bekker, A., Holland, H. D., Wang, P. L., Rumble, D., Stein, H. J., Hannah, J. L., Coetzee, L. L. & Beukes, N. J. 2004 Dating the rise of atmospheric oxygen. *Nature* **427**, 117–120. (doi:10.1038/nature02260)

Berman-Frank, I., Lundgren, P. & Falkowski, P. 2003 Nitrogen fixation and photosynthetic oxygen evolution in cyanobacteria. *Res. Microbiol.* **154**, 157–164. (doi:10.1016/S0923-2508(03)00029-9)

Berner, R. A. 1980 *Early diagenesis: a theoretical approach.* Princeton, NJ: Princeton University Press.

Boetius, A. *et al.* 2000 A marine microbial consortium apparently mediating anaerobic oxidation of methane. *Nature* **407**, 623–626. (doi:10.1038/35036572)

Borowski, W. S., Paull, C. K. & Ussler, W. 1996 Marine pore-water sulfate profiles indicate *in situ* methane flux from underlying gas hydrate. *Geology* **24**, 655–658. (doi:10.1130/0091-7613(1996)024<0655:MPWSPI>2.3.CO;2)

Borowski, W. S., Paull, C. K. & Ussler, W. 1999 Global and local variations of interstitial sulfate gradients in deep-water, continental margin sediments: sensitivity to underlying methane and gas hydrates. *Mar. Geol.* **159**, 131–154. (doi:10.1016/S0025-3227(99)00004-3)

Brocks, J. J., Buick, R., Summons, R. E. & Logan, G. A. 2003 A reconstruction of Archean biological diversity based on molecular fossils from the 2.78 to 2.45 billion-year-old Mount Bruce Supergroup, Hamersley Basin, Western Australia. *Geochim. Cosmochim. Acta* **67**, 4321–4335. (doi:10.1016/S0016-7037(03)00209-6)

Canfield, D. E. 1991 Sulfate reduction in deep-sea sediments. *Am. J. Sci.* **291**, 177–188.

Canfield, D. E. 2005 The early history of atmospheric oxygen: homage to Robert A. Garrels. *Annu. Rev. Earth Planet. Sci.* **33**, 1–36. (doi:10.1146/annurev.earth.33.092203.122711)

Canfield, D. E., Habicht, K. S. & Thamdrup, B. 2000 The Archean sulfur cycle and the early history of atmospheric oxygen. *Science* **288**, 658–661. (doi:10.1126/science.288.5466.658)

Canfield, D. E., Poulton, S. W. & Narbonne, G. M. 2007 Late-Neoproterozoic deep-ocean oxygenation and the rise of animal life. *Science* **315**, 92–95. (doi:10.1126/science.1135013)

Catling, D. C. & Claire, M. W. 2005 How Earth's atmosphere evolved to an oxic state: a status report. *Earth Planet. Sci. Lett.* **237**, 1–20. (doi:10.1016/j.epsl.2005.06.013)

Catling, D. C., Zahnle, K. J. & McKay, C. P. 2001 Biogenic methane, hydrogen escape, and the irreversible oxidation of early Earth. *Science* **293**, 839–843. (doi:10.1126/science.1061976)

Catling, D. C., Claire, M. W. & Zahnle, K. J. 2004 Understanding the evolution of atmospheric redox state from the Archaean to the Proterozoic. In *Field forum on processes on the early Earth* (eds W. U. Reimold & A. Hofmann), pp. 17–19. Kaapvaal Craton, South Africa: University of Witwatersrand.

Claire, M. W., Catling, D. C. & Zahnle, K. J. 2006 Biogeochemical modeling of the rise of oxygen. *Geobiology* **4**, 239–269. (doi:10.1111/j.1472-4669.2006.00084.x)

Devol, A. H. 1983 Methane oxidation rates in the anaerobic sediments of Saanich Inlet. *Limnol. Oceanogr.* **28**, 738–742.

Eyles, N. 1993 Earths glacial record and its tectonic setting. *Earth-Sci. Rev.* **35**, 1–248. (doi:10.1016/0012-8252(93)90002-O)

Farquhar, J., Bao, H. & Thiemans, M. 2000 Atmospheric influence of Earth's earliest sulfur cycle. *Science* **289**, 756–758. (doi:10.1126/science.289.5480.756)

Fike, D. A., Grotzinger, J. P., Pratt, L. M. & Summons, R. E. 2006 Oxidation of the Ediacaran Ocean. *Nature* **444**, 744–747. (doi:10.1038/nature05345)

Garrels, R. M. & Perry, E. A. 1974 Cycling of carbon, sulfur and oxygen through geological time. In *The sea* (ed. E. D. Goldberg), pp. 303–316. New York, NY: Wiley Interscience.

Goldblatt, C., Lenton, T. M. & Watson, A. J. 2006 Bistability of atmospheric oxygen and the Great Oxidation. *Nature* **443**, 683–686. (doi:10.1038/nature05169)

Habicht, K. S., Gade, M., Thamdrup, B., Berg, P. & Canfield, D. E. 2002 Calibration of sulfate levels in the Archean ocean. *Science* **298**, 2372–2374. (doi:10.1126/science.1078265)

Haese, R. R., Meile, C., Van Cappellen, P. & De Lange, G. J. 2003 Carbon geochemistry of cold seeps: methane fluxes and transformation in sediments from Kazan mud volcano, eastern Mediterranean sea. *Earth Planet. Sci. Lett.* **212**, 361–375. (doi:10.1016/S0012-821X(03)00226-7)

Hayes, J. M. 1994 In *Global methanotrophy at the Archean–Preoterozoic transition* (ed. S. Bengtson), pp. 220–236. New York, NY: Columbia University Press.

Hayes, J. M. & Waldbauer, J. R. 2006 The carbon cycle and associated redox processes through time. *Phil. Trans. R. Soc. B* **361**, 931–950. (doi:10.1098/rstb.2006.1840)

Hinrichs, U. 2002 Microbial fixation of methane carbon at 2.7 Ga: was an anaerobic mechanism responsible? *Geol. Geochem. Geophys.* **3**, 1042. (doi:10.1029/2001GC000286)

Hinrichs, K. U. & Boetius, A. 2002 The anaerobic oxidation of methane: new insights in microbial ecology and biogeochemistry. In *Ocean margin systems* (eds G. Wefer, D. Billett, D. Hebbeln, B. B. Jorgensen, M. Schluter & T. Van Weering), pp. 457–477. Berlin, Germany: Springer.

Holland, H. D. 1978 *The chemistry of the atmosphere and oceans*. New York, NY: Wiley.

Holland, H. D. 2002 Volcanic gases, black smokers, and the Great Oxidation Event. *Geochim. Cosmochim. Acta* **66**, 3811–3826. (doi:10.1016/S0016-7037(02)00950-X)

Ingvorsen, K. & Brock, T. D. 1982 Electron flow via sulfate reduction and methanogenesis in the anaerobic hypolimnion of Lake Mendota. *Limnol. Oceanogr.* **27**, 559–564.

Iversen, N. & Jorgensen, B. B. 1985 Anaerobic methane oxidation rates at the sulfate methane transition in marine-sediments from Kattegat and Skagerrak (Denmark). *Limnol. Oceanogr.* **30**, 944–955.

Iversen, N. & Jorgensen, B. B. 1993 Diffusion coefficients of sulfate and methane in marine sediments: influence of porosity. *Geochim. Cosmochim. Acta* **57**, 571–578. (doi:10.1016/0016-7037(93)90368-7)

Jorgensen, B. B., Bottcher, M. E., Luschen, H., Neretin, L. N. & Volkov, I. I. 2004 Anaerobic methane oxidation and a deep H2S sink generate isotopically heavy sulfides in Black Sea sediments. *Geochim. Cosmochim. Acta* **68**, 2095–2118. (doi:10.1016/j.gca.2003.07.017)

Kah, L. C., Lyons, T. W. & Frank, T. D. 2004 Low marine sulphate and protracted oxygenation of the Proterozoic biosphere. *Nature* **431**, 834–838. (doi:10.1038/nature02974)

Kasting, J. F. & Howard, M. T. 2006 Atmospheric composition and climate on the early Earth. *Phil. Trans. R. Soc. B* **361**, 1733–1741. (doi:10.1098/rstb.2006.1902)

Kruger, M., Treude, T., Wolters, H., Nauhaus, K. & Boetius, A. 2005 Microbial methane turnover in different marine habitats. *Palaeogeogr. Palaeoclimatol. Palaeoecol.* **227**, 6–17. (doi:10.1016/j.palaeo.2005.04.031)

Luff, R. & Wallmann, K. 2003 Fluid flow, methane fluxes, carbonate precipitation and biogeochemical turnover in gas hydrate-bearing sediments at Hydrate Ridge, Cascadia Margin: numerical modeling and mass balances. *Geochim. Cosmochim. Acta* **67**, 3403–3421. (doi:10.1016/S0016-7037(03)00127-3)

Martens, C. S. & Berner, R. A. 1977 Interstitial water chemistry of anoxic Long Island Sound sediments. 1. Dissolved gases. *Limnol. Oceanogr.* **22**, 10–25.

Middelburg, J. J., Soetaert, K. & Herman, P. M. J. 1997 Empirical relationships for use in global diagenetic models. *Deep-Sea Res. Part I-Oceanogr. Res. Papers* **44**, 327–344. (doi:10.1016/S0967-0637(96)00101-X)

Ono, S., Eigenbrode, J. L., Pavlov, A. A., Kharecha, P., Rumble III, D., Kasting, J. F. & Freeman, K. H. 2003 New insights into Archean sulfur cycle from mass-independent sulfur isotope records from the Hamersley Basin, Australia. *Earth Planet. Sci. Lett.* **213**, 15–30. (doi:10.1016/S0012-821X(03)00295-4)

Patchett, P. J. & Arndt, N. T. 1986 Nd isotopes and tectonics of 1.9–1.7 Ga crustal genesis. *Earth Planet. Sci. Lett.* **78**, 329–338. (doi:10.1016/0012-821X(86)90001-4)

Pavlov, A. A. & Kasting, J. F. 2002 Mass-independent fractionation of sulfur isotopes in Archean sediments: strong evidence for an anoxic Archean atmosphere. *Astrobiology* **2**, 27–41. (doi:10.1089/153110702753621321)

Pavlov, A. A., Kasting, J. F., Brown, L. L., Rages, K. A. & Freedman, R. 2000 Greenhouse warming by CH_4 in the atmosphere of early Earth. *J. Geophys. Res.* **105**, 11 981–11 990. (doi:10.1029/1999JE001134)

Pavlov, A. A., Kasting, J. F. & Brown, L. L. 2001 UV-shielding of NH_3 and O_2 by organic hazes in the Archean atmosphere. *J. Geophys. Res.* **106**, 23 267–23 287. (doi:10.1029/2000JE001448)

Pavlov, A. A., Hurtgen, M. T., Kasting, J. F. & Arthur, M. A. 2003 Methane-rich Proterozoic atmosphere? *Geology* **31**, 87–90. (doi:10.1130/0091-7613(2003)031<0087:MRPA>2.0.CO;2)

Prather, M. *et al.* 2001 Atmospheric chemistry and greenhouse gases. In *Climate change 2001, the scientific basis* (eds J. T. Houghton, Y. Ding, D. J. Griggs, M. Noguer, P. J. van der Linden, X. Dai, K. Maskell & C. A. Johnson), pp. 239–287. Cambridge, UK: Cambridge University Press.

Raghoebarsing, A. A. *et al.* 2006 A microbial consortium couples anaerobic methane oxidation to denitrification. *Nature* **440**, 918–921. (doi:10.1038/nature04617)

Reeburgh, W. S. 1976 Methane consumption in cariaco trench waters and sediments. *Earth Planet. Sci. Lett.* **28**, 337–344. (doi:10.1016/0012-821X(76)90195-3)

Reeburgh, W. S. 1996 "Soft Spots" in the global methane budget. In *Microbial growth on C1 compounds* (eds M. E. Linstrom & F. R. Tabita), pp. 334–342. Dordrecht, The Netherlands: Kluwer.

Reeburgh, W. S. & Heggie, D. T. 1977 Microbial methane consumption reactions and their effect on methane distributions in freshwater and marine environments. *Limnol. Oceanogr.* **22**, 1–9.

Rogers, J. J. W. & Santosh, M. 2004 *Continents and supercontinents*. New York, NY: Oxford University Press.

Shen, Y., Knoll, A. H. & Walter, M. R. 2003 Evidence for low sulphate and anoxia in a mid-Proterozoic marine basin. *Nature* **423**, 632–635. (doi:10.1038/nature01651)

Summons, R. E., Bradley, A. S., Jahnke, L. L. & Waldbauer, J. R. 2006 Steroids, triterpenoids and molecular oxygen. *Phil. Trans. R. Soc. B* **361**, 951–968. (doi:10.1098/rstb.2006.1837)

Valentine, D. L. 2002 Biogeochemistry and microbial ecology of methane oxidation in anoxic environments: a review. *Antonie Van Leeuwenhoek Int. J. Gen. Mol. Microbiol.* **81**, 271–282. (doi:10.1023/A:1020587206351)

Van Cappellen, P. & Wang, Y. F. 1996 Cycling of iron and manganese in surface sediments: a general theory for the coupled transport and reaction of carbon, oxygen, nitrogen, sulfur, iron, and manganese. *Am. J. Sci.* **296**, 197–243.

Walker, J. C. G. 1980 The oxygen cycle. In *The natural environment and the biogeochemical cycles* (ed. O. Hutzinger), pp. 87–104. Berlin, Germany: Springer.

Walker, J. C. G. & Brimblecombe, P. 1985 Iron and sulfur in the pre-biologic ocean. *Precambrian Res.* **28**, 205–222. (doi:10.1016/0301-9268(85)90031-2)

Walker, J. C. G., Klein, C., Schidlowski, M., Schopf, J. W., Stevenson, D. J. & Walter, M. R. 1983 Environmental evolution of the Archean-early Proterozoic Earth. In *Earth's earliest biosphere: its origin and evolution* (ed. J. W. Schopf), pp. 260–290. Princeton, NJ: Princeton University Press.

Wallmann, K., Drews, M., Aloisi, G. & Bohrmann, G. 2006 Methane discharge into the Black Sea and the global ocean via fluid flow through submarine mud volcanoes. *Earth Planet. Sci. Lett.* **248**, 545–560. (doi:10.1016/j.epsl.2006.06.026)

Warneck, P. 2000 *Chemistry of the natural atmosphere*. New York, NY: Academic Press.

Whiticar, M. J. 2002 Diagenetic relationships of methanogenesis, nutrients, acoustic turbidity, pockmarks and freshwater seepages in Eckernforde Bay. *Mar. Geol.* **182**, 29–53. (doi:10.1016/S0025-3227(01)00227-4)

Zahnle, K., Claire, M. & Catling, D. 2006 The loss of mass-independent fractionation in sulfur due to a Paleoproterozoic collapse of atmospheric methane. *Geobiology* **4**, 271–283. (doi:10.1111/j.1472-4669.2006.00085.x)